Pramana – J. Phys. (2020) 94:66
https://doi.org/10.1007/s12043-020-1934-9

Design and calibration of a passive detector for separating neutron, proton and α-particles in mixed radiation fields

FARBOD BAHRAMI[1], SAMANEH BARADARAN[2,3,*], MEHRAN TAHERI[3] and FEREIDOUN MIANJI[2,3]

[1]Department of Medical Radiation Engineering, Shiraz University, Shiraz 71964 84334, Iran
[2]Nuclear Science and Technology Research Institute, Tehran 14399 836, Iran
[3]National Radiation Protection Department, Iran Nuclear Regulatory Authority, Tehran 14155 1339, Iran
*Corresponding author. E-mail: sbaradaran@aeoi.org.ir

MS received 2 December 2018; revised 11 December 2019; accepted 21 January 2020

Abstract. In this study, a new detector is designed based on CR-39, and separately calibrated for protons, neutrons and α-particles under the same etching condition. To that end, an americium–beryllium standard source (^{241}Am–Be) and a plexiglass phantom for neutron irradiation, brass collimators and an americium standard source (^{241}Am) for alpha irradiation, as well as a Van de Graaff accelerator for proton irradiation were employed. Sodium hydroxide solution of 6.25 N at 85°C was also used for CR-39 chemical etching. Considering the detection principle of the device, different filters were designed to help distinguish between fast neutron particles, thermal neutrons, albedo neutrons, protons and α-particles in mixed radiation fields. Moreover, both the contribution of each particle and the ability of the designed detector to discriminate energy of charged particles were quantified.

Keywords. CR-39 solid-state nuclear track detector; track detection; mixed radiation field; calibration.

PACS Nos **29.40.Wk; 87.57.uq; 29.40.−n**

1. Introduction

Solid-state nuclear track detector (SSNTD) is a type of passive detector whose working principle is based on breakages in the chain of its structural monomers leading to the creation of tracks along the path of the particles. Latent tracks will appear after a particular time by undergoing a chemical etching process with etching solutions such as NaOH or KOH, and these tracks can be evaluated by an optical microscope. Properties like high uniformity in response, high recording efficiency, low cost, sensitivity to high LET particles, and being of little sensitivity to γ-rays are remarkable characteristics of SSNTD. Poly-allyl-diglycol-carbonate (PADC) is an SSNTD track detector that is commercially known as CR-39 [1]. It has been employed in neutron dosimetry, passive spectrometry of alpha and neutron, radon dosimetry, space radiation dosimetry for technical staff and aircraft crew, airplanes and satellite shields radiation monitoring etc. [2–6]. CR-39 track etch detector can be used for proton beam dosimetry in radiotherapy and it can also record recoil protons induced from neutrons, which can be useful for dosimetric applications [7, 8]. Nowadays the use of passive detectors is more common due to possible difficulties and specific limitations of active detectors in particular circumstances. There exist various methods for particle separation including the time-of-flight technique, pulse-shaped separation by plastic scintillators and Phoswich detectors [9–12]. Sohrabi and Katouzi [13] designed a CR-39 dosimeter commercially known as NANPD that can discriminate fast, thermal and albedo neutrons. Majeed *et al* [14] have used three different track etch detectors (PC, CR-39 and CN-85) to record α-particle, proton particle and recoil nucleus. Sadowski *et al* [15] designed a detector which can record proton particles only with 0.2−1.6 MeV energy range while it was not able to record higher energies. Bahrami *et al* [16] introduced a new method (based on high etching temperature) and could record proton particles up to 2.5 MeV with lesser etching time than that of Sadowski research. The main purpose of this study was to design a dosimeter with the possibility of simultaneously detecting different types of nuclear radiation in the mixed radiation fields instead of using multiple dosimeters. The radiation energy used in this study was mainly related to the most common

Published online: 16 April 2020

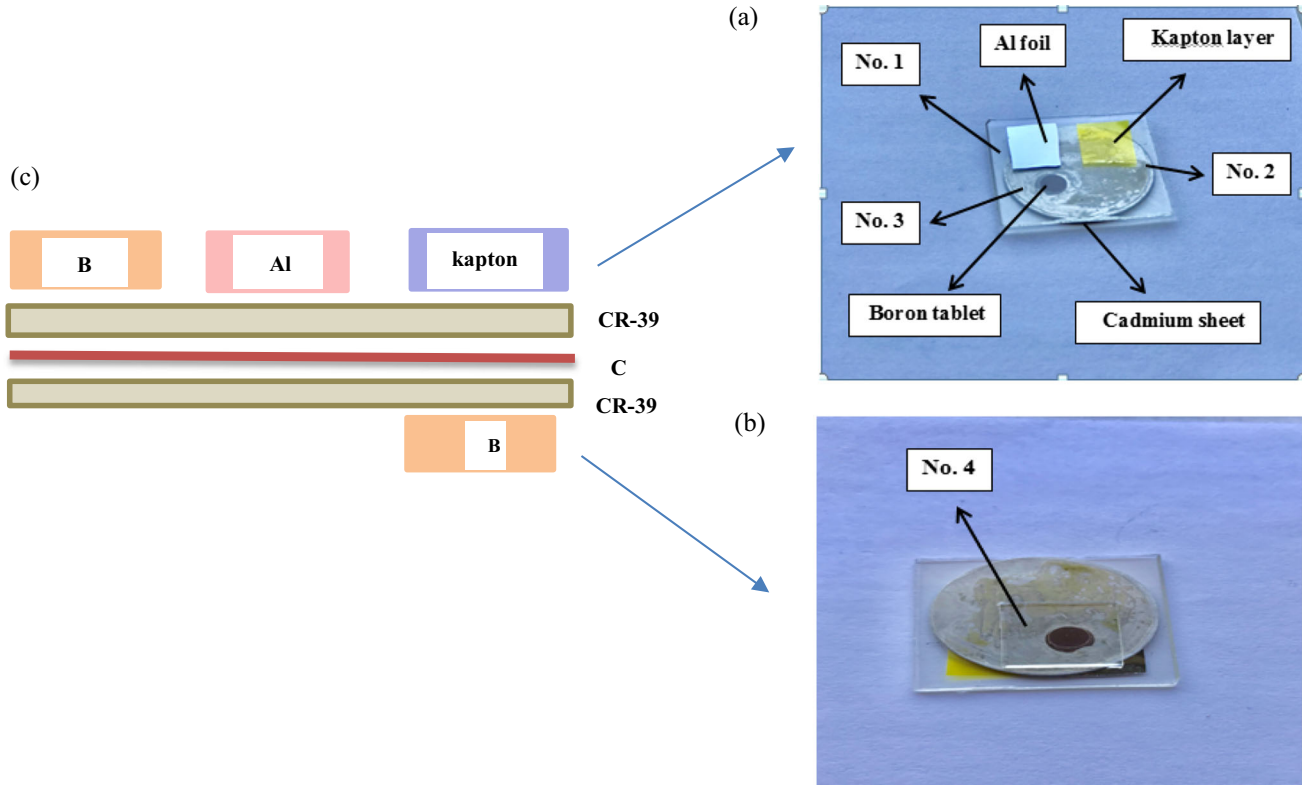

Figure 1. Designed detector including ROIs, boron tablet, cadmium sheet and shields is depicted. (**a**) The film with ROIs is on the cadmium sheet, (**b**) the film is under the cadmium sheet and (**c**) the schematics of the designed detector.

range of energy in various activities involving nuclear radiation. Given the facilities at hand, the energy range of the α-particles is up to 5.48 MeV (standard ^{241}Am source), that of the proton particles is 0.9 MeV−2.5 MeV and the neutron energy is for the standard ^{241}Am−Be source with the mean value of 4.5 MeV. Designing this dosimeter by using SSNTD-CR39 is an innovation of its kind and it can be developed to evaluate occupational or environmental exposure.

2. Materials and methods

The designed detector, as shown in figure 1, consists of four ROIs (regions of interst) on two pieces of CR-39 detector. Factors taken into consideration include optimised geometric factors, proper composition of components and the use of appropriate filters to separately record protons, neutrons and α-particles in mixed radiation fields. It comprises CR-39 detectors, boron tablets and cadmium cover with optimum thicknesses, kapton and aluminum layers. To construct a discriminator detector, eight CR-39 detectors were categorised in two groups of four and were prepared for two distinct series of exposure. The designed detector, as shown in figure 1, consists of three CR-39 track detectors (1 cm × 1 cm). Optimised geometric factors, proper composition of components and using appropriate filters to separately record protons, neutrons and α-particles in mixed radiation fields are considered [16].

In figure 1, the regions 1, 2, 3 and 4 correspond respectively to: 45 μm thick aluminum placed on the detector, 7.5 μm thick kapton layer placed on the detector, a boron tablet mounted on a cadmium sheet placed on the detector and boron tablet mounted below the cadmium sheet placed on the detector.

Please note that the cadmium sheet includes two boron tablets mounted on each side and is placed between the two detectors.

In order to calibrate the detector for proton, neutron and α-particles, the following sources were used respectively: Van de Graaff accelerator of AEOI, and ^{241}Am−Be and ^{241}Am sources. All the CR-39 detectors with 750 μm thickness and the size of 1 cm × 1 cm were categorised and specified in four groups to detect the three types of particles in different energies. After the exposure, they were chemically etched by 6.25 N NaOH at 85°C. Experimental set-up for CR-39 calibration to each particle is demonstrated in figure 2.

2.1 *Exposing CR-39 samples to proton particle*

Due to the particular Van de Graaff circumstances, direct exposure of the detectors by proton beam was not applicable. Therefore, a uniform pure Au foil of 800 nm thickness and 7 mm diameter were used for the experiments (the elastic collision of the primary protons with the Au foil results in 4π scattering). The protons that reached the samples, known as Rutherford backscattering protons, were almost mono-energetic. Calculations by SIMNRA software [17] showed that the energy loss of the backscattered protons for all energy range of the accelerator was less than 40 keV; so energies of the backscattered protons were assumed to be equal to that of the primary beam. Since generating specific proton energies was not accessible through the device direct adjustment, one or more kapton-polyimide films ($C_{22}H_{10}N_2O_5$) of 7.5 μm thickness were placed on the CR-39 detectors (figure 2b). The TRIM software was employed to calculate the energy reduction of protons by the layer(s). In order to minimise statistical uncertainties, five samples (the geometry of the experiments limited the number of samples) were placed in the device for each proton's energy. The Van de Graaff current was set on 4 nA and the pressure was reduced to 10^{-4} Torr in all the experiments. A surface barrier detector was employed to control each step of the exposure to ensure the correctness and stability of the proton flux. The detector was placed exactly under the samples at 165° angle respecting the primary beam. To eliminate the ambient light noise, the surface of the barrier detector was protected (covered) against light by a tube. The proton energies employed were 0.94, 1.1, 1.5, 1.7, 1.85, 2 and 2.5 MeV (35 samples totally). The upper energy limit was imposed by the Van de Graaff accelerator's operating range. In order to avoid possible track overlapping and also difficulties in reading CR-39 detectors, all samples were exposed to 2.5×10^4 cm^{-2} proton fluence. Afterwards, the samples etched about 1.5 h, were put under optical microscope for the initial evaluation of track diameters and were analysed by automatic track counting system [16].

2.2 *Exposing CR-39 samples to neutron particle*

In this study, the neutron irradiation was carried out by americium–beryllium standard source (^{241}Am–Be) with an emission rate of 1.96×10^7 n/s. A boron tablet was used to convert thermal and albedo neutrons (returned from the body) to α-particles because this detector is not sensitive to thermal neutrons and boron has a high thermal neutron cross-section. However, the detector is sensitive to fast neutrons too. The thickness and diameter of the boron were 7.5 mg/cm^2 and 8 mm. In larger thicknesses, the number of impinged α-particles on the detector decreased because of boron self-absorption. If the thickness was not optimised, the number of impinged α-particles to the detector could not be uniform [13]. To detect the albedo neutrons produced by the fast neutron collision to the water phantom,

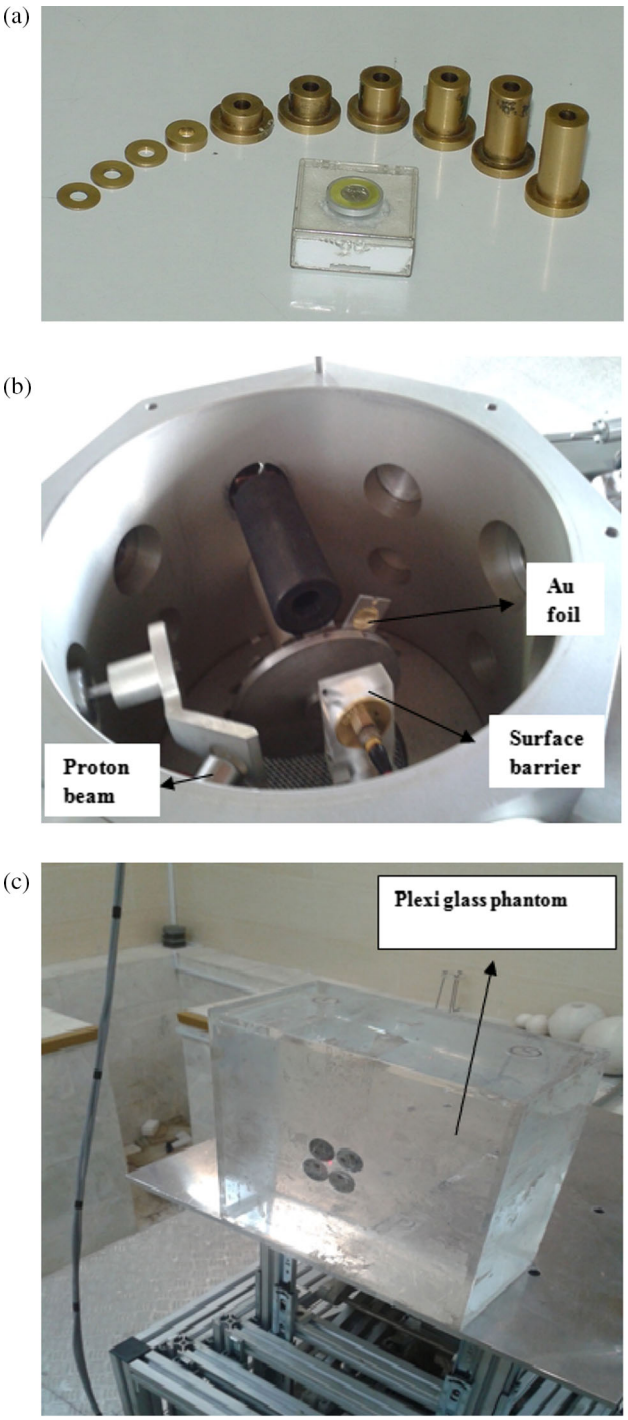

Figure 2. Experimental set-up for CR-39 exposing to (**a**) α-particles with ^{241}Am source, (**b**) proton particles with accelerator and (**c**) neutron particles with ^{241}Am–Be source.

a cadmium cover was used to prevent thermal neutrons from the head-on side. The phantom used in this study was made of standard plexiglass with the surface of 30 cm × 30 cm and was filled with water (figure 2c). At dosimeter–source distance of 40 cm, the relative neutron response is increased up to 20% by increasing the dosimeter–phantom distance by 1 cm. This trend reached a maximum and then decreased again. Accordingly, the detectors were attached to the phantom with adhesive tapes and were placed at a distance of 0.5 m from the Am−Be source. Afterwards, the centre of the phantom was adjusted (arranged) by a laser light and then four samples on four sides of the centre in phantom were placed and exposed [18]. CR-39 detectors were exposed by doses of 5, 20 and 50 mSv. The background radiation was also subtracted for the calculated tracks related to each dose.

2.3 *Exposing CR-39 samples to α-particles*

The samples exposed to α-particles by ^{241}Am were etched for an interval of 1.5 h. Considering alpha irradiation effects, alpha energy of 5.48 MeV (^{241}Am as the source) was used to expose the detectors. The energy of α-particles impinging on the detector drops while travelling in the air at atmospheric pressure. In other words, the spectrum of α-particles reaching the detector is significantly dependent on the distance between the source and the detector (brass collimators with various heights as seen in figure 2a).

2.4 *Reading out the etched tracks of CR-39*

In NRPD dosimetry and detection laboratory, a comprehensive automatic track counting system is used to analyse nuclear particle tracks in SSNTDs. This system consists of a high-resolution digital image convertor with a transparency adapter and an image processing and analyser program. According to the experimental investigations, the linearity of track density response for the increase in radiation exposure is reliable up to 10^4 tracks cm^{-2} [19]. After the chemical etching of CR-39 samples, they were automatically counted and the results were evaluated.

3. Results and discussion

Figure 3 shows the track diameter as a function of etching time for different proton energies. Formation of tracks through chemical etching is a function of two variables: (1) the etch rate along the track (V_t) and (2) the bulk etch rate of the track detector (V_b). These variables are related to the etching parameters through eqs

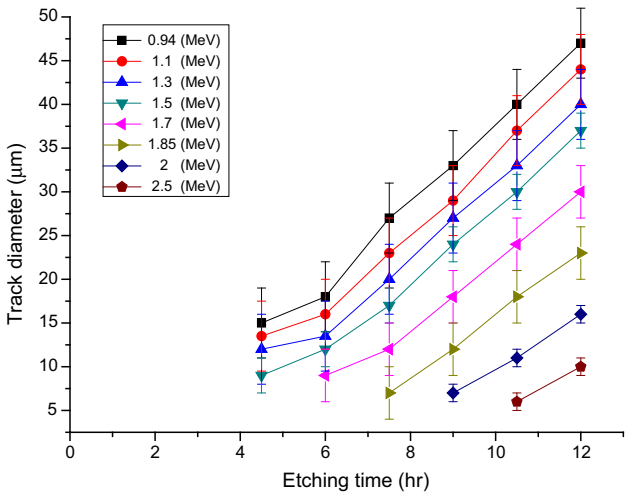

Figure 3. Response of the CR-39 detectors to different proton energies at various etching times in NaOH etching solution (6.25 N and 85 ± 1°C) [16].

(1) and (2) proposed for tracks of α-particles in CR-39. The relations are employed here for protons (V_b is in fact independent on the particle type) where h is the thickness of the removed surface of the detector during the etching period, t is the etching time and d is the particle track diameter at normal incidence [16,18].

$$V_b = \frac{h}{t} \tag{1}$$

$$V = \frac{(1+r^2)}{(1-r^2)}, \quad r = \frac{d}{2h}, \quad V_t = \frac{V}{V_b}. \tag{2}$$

As higher energy protons can break the polymer chain in deeper layers, more etching time is required to reach these leayers for track formation and consequently tracks appear later. So higher proton energies have smaller track diameters. It can also be expanded to track etch rate and bulk etch rate; the lower their rates are, the lower will be the track diameters for proton particles [16]. Figure 4 shows the track etch rate (V_t) as a function of proton energy and it can be seen that V_t decreases as the proton energy increases.

Based on the result of exposed detectors with neutron particles, contribution of the fast neutrons was calculated and the calibration curve is shown in figure 5.

The ^{241}Am−Be(α, n) source is known as the fast neutron source. Therefore, the CR-39 detectors were exposed by this source with a mean energy of 4.5 MeV in different doses.

The four points shown in figure 5 are indicators as to the number of tracks in each dose of neutron exposure.

Results of CR-39 calibration for various alpha energies are depicted in figure 6. The behaviour of etching rate for α-particle is shown in figure 7. The results reveal that longer etching time can be the extended energy

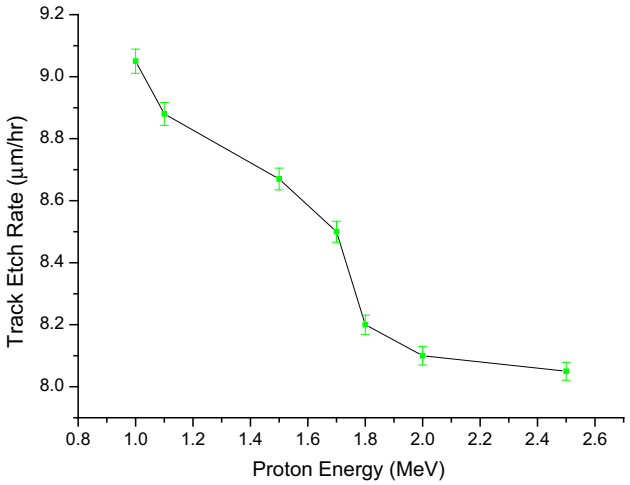

Figure 4. Track etch rate (μm/h) vs. proton energy (MeV) in CR-39 for final etching time (12 h) in NaOH etching solution (6.25 N and 85 ± 1°C) [16].

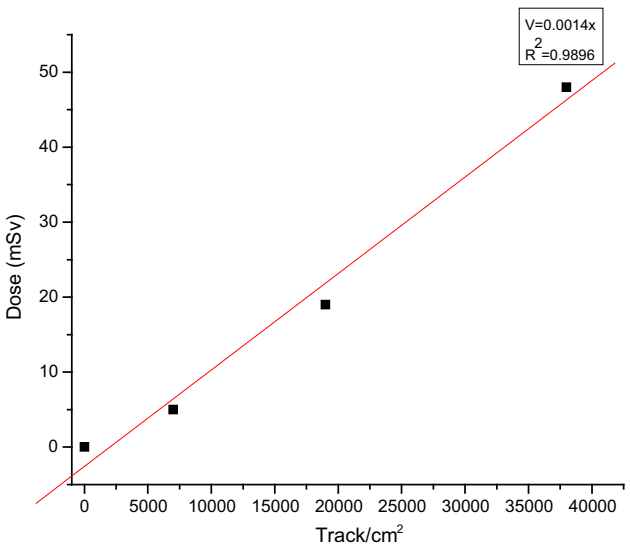

Figure 5. The calibration curve of the fast neutrons in the ^{241}Am–Be field over 5 h of etching in NaOH (6.25 N and 85 ± 1°C).

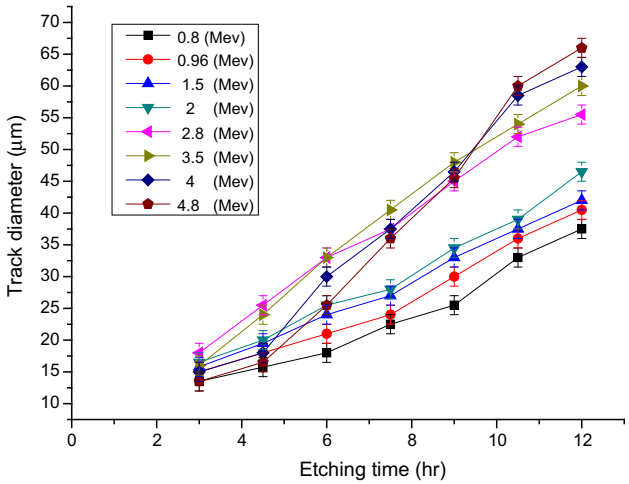

Figure 6. The response of CR-39 film for α-particles during different etching times vs. different energies in NaOH (6.25 N and 85 ± 1°C).

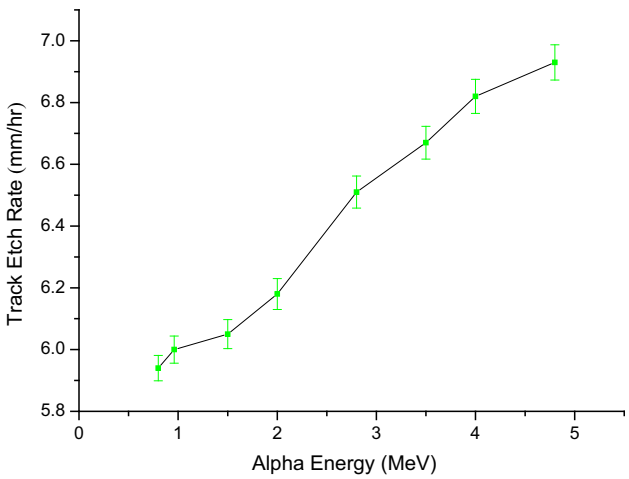

Figure 7. Track etch rate vs. alpha energy in CR-39 for the final etching time (12 h) in NaOH (6.25 N and 85 ± 1°C).

detection range for α-particles. Totally, it was observed that the track diameter increases by the etching time in all stages.

According to the achieved results, a detector was designed (figure 1) for identifying α-, proton and neutron particles. As shown in figure 1, this detector is designed to initially detect 1.5 MeV protons, 1 MeV α-particles emanated from ^{241}Am source (using a brass collimator) and finally neutrons of ^{241}Am–Be source with the dose of 4 mSv. In this set-up, two layers of copper were used to stop α-particles. All samples were chemically etched for 5 h in 6.25 N NaOH etching solution (6.25 N and 85 ± 1°C). In the second set, the detectors were sequentially exposed by 1.2 MeV protons, 1.5 MeV alpha induced by ^{241}Am (using brass collimator) and neutrons of ^{241}Am–Be source with the dose of 4 mSv. All samples were chemically etched as mentioned above. In this series, a layer of copper was used to stop α-particles. It was assumed that there is no information about the numbers, energy and the types of particles. All particles can be recorded by the detector in region 3, and so the detector records a mixture effect of all particles (protons, neutrons and alpha). Therefore, all the particles will be recorded in all areas of the detector, except the region where boron is located. Alpha and proton particles cannot pass through boron because of their short range through boron. Boron can absorb thermal neutron and emit α-particles, which are different from the α-particles

Table 1. Track density in different areas of the designed detector in radiation fields and determination the energy of particles.

First series	Mixed field	Second series	Mixed field
Alpha tracks/cm^2	8583	Alpha tracks/cm^2	6708
Proton tracks/cm^2	12958	Proton tracks/cm^2	14208
Albedo neutron tracks/cm^2	2068	Albedo neutron tracks/cm^2	2176
Fast neutron tracks/cm^2	4208	Fast neutron tracks/cm^2	4270
Thermal neutron tracks/cm^2	207	Thermal tracks/cm^2	334

Table 2. Separating the particle types and determining the number of particles in the designed detector.

First series	Mixed field	Second series	Mixed field
Total tracks in cm^2 (region No.3)	28125	Total tracks in cm^2 (region No.3)	27500
Total tracks in cm^2 (region No.2)	18750	Total tracks in cm^2 (region No.2)	20000
Total tracks in cm^2 (region No.1)	5000	Total tracks in cm^2 (region No.1)	5000
Alpha track diameter (μm)	17	Alpha track diameter (μm)	22
Proton track diameter (μm)	17	Proton track diameter (μm)	15

emitted from the Am source. In region 2, the thickness of the kapton layer will prevent α-particles (considering the TRIM software calculations). Vacuum during the irradiation causes the complete attachment of the kapton layer to CR-39. Due to this, the energy of all proton particles will drop before they reach the detector surface which means that this decrement amount can be calculated by the TRIM software and incidence energy can obtained. According to the differences between region 3 (which has recorded all the particles) and region 2 (which has recorded neutron and proton), the number of α-particles can be determined. In region 1, a 45 μm thick aluminum foil was used. The distance between the aluminum foil and CR-39 is 1.5 mm which means that neutron particles pass only from this layer, and this minor air gap does not have any effect for these particles to reach CR-39. According to the calculations, such a thickness can stop α- and proton particle tracks with beforementioned energies. Thus, there are only neutrons in this area (region 1). According to the difference between regions 1 and 2, the number of protons can be obtained. Having done the separation of particles, fast neutron dose, proton and α-particle energies can be calculated due to the calibration process. For instance, by means of region 2 (which detect only proton and neutron tracks), proton energy can be determined by using mean track diameter and calibration curve, owing to fairly equal track diameter of protons. Proton and alpha spectrometry can be achieved by track detection in different etching times (multistage etching); the required time to detect different energy of proton and α- particles is attainable as well. In addition, requirements for calibration condition in the NaOH etching solution (6.25 N, 85 $\pm$ 1°C), urge all films to be etched alike, nearly 5 h at 85° C. Regarding the region No. 3 which records all particles, the energy of α-particles can be determined by removing the background track as shown in figure 5. In tables 1 and 2, the region No. 1 is a detector in which all particles are recorded (without shield), while region No. 2 is a detector in which proton and neutron are recorded (using kapton layer) and in region No. 1 only neutron particle is recorded (using the aluminum foil). The track diameter of α-particle has a considerable correlation with the results of alpha calibration curve. Considering the track diameter of the proton particle (when there are two layers of kapton in the first series of irradiation), a 24-μm diameter pertaining to the energy of 1.15 MeV was achieved. It was confirmed by the TRIM results. So the energy of the proton particles which reached the detector surface is 1.5 MeV. In the second series, the diameter of proton particle is 15 μm, and with a kapton layer, its energy is 1.2 MeV. Considering the TRIM results, the energy of protons in the presence of this layer is 1.2 MeV too. Hence, based on the results, the number of α-, proton and neutron particles can be easily found by subtracting film counts from each other. There are only neutron particles in the aluminum layer and also the boron pellet. Under this region, there are only thermal neutrons from the front and outside of this region and as a result, only fast neutrons have been detected. The difference between counts in these two areas gives the number of thermal neutrons. The number of Albedu's neutrons can be determined by region No. 4 which is located behind cadmium and on the phantom in figure 2. The same scenario happens for Albedu's neutrons as mentiond for thermal neutrons. As mentioned in table 1, the flux of 5×10^3 track /cm^2 (the hit number of neutron particles) is related to 4 mSv dose. This fact

verifies the accuracy of the fast neutron calibration curve (figure 5). Although the number of impinged particles is equal in each two series, the variance of recording particles can be considered as the statistical nature of radiation. Finally, particles discrimination (by the subtraction of background radiation) and energy separation for proton and alpha are presented in table 2. Tracks related to backgound radiation is subtracted from the calculated tracks in all areas. The designed detector can be used by radiation workers (installed on the chest) in mixed fields. If it is not possible to place the detector on a radiation worker's body, the detector can be installed on something like water tanks (because human body consist of approximately 80% of water). If there are high energy and flux of charged particles nearby, this detector-discriminator provides monitoring/protective tasks. It is also feasible to place such a tool on airplanes and satellites to estimate the hit number (for neutron, proton, alpha) and consequently to protect personnel and electronic components. It is productive to add a shielding material if necessary.

4. Conclusion

This research presents a detector with an appropriate combination of materials and various filters to provide an approach for the discrimination of protons, α-, fast neutron, thermal neutron and albedo neutron particles, as well as separation of the energy of proton and α-particles. The results of proton irradiation (Van de Graff accelerator) show that proton radiation spectrometry is achievable by taking samples off in an etching time of 1.5 h. It is obvious that due to various energies, proton tracks can be distinguished at different etching times and etching solutions. Regarding proton exposer with the energy range of 0.94−2.5 MeV, it is shown that track diameter decreases when proton energy increases and the track diameter also increases as etching time extends. The results of the samples exposed to α-particles reveal that better energy discrimination can be obtained for longer etching duration. Eventually, this work provides the calibration information that can be used in unknown mixed radiation fields.

References

[1] D Nikezic and K N Yu, *Mater. Sci. Eng. Rep*. **46**, 51 (2004)
[2] F Castillo, G Espinosa, J I Golzarri, D Osorio, P G Reyes and J J E Herrera, *Radiat. Meas*. **50**, 71 (2013)
[3] D Fan, W Zhuo, B Chen, C Zhao, Y Yi and Y Zhang, *Rad. Prot. Dosim*. **167**, 1 (2015)
[4] S Paul, S P Tripathy, G S Sahoo, T Bandyopadhyay and P K Sarkar, *Nucl. Instrum. Methods Phys. Res.* **729**, 444 (2013)
[5] M E Ghazaly, *Radiat. Eff. Def.* **167**, 421 (2012)
[6] S Kodaira, R V Tolochek, I Ambrozova, H Kawashima, N Yasuda and M Kurano. *Adv. Space Res*. **53**, 1 (2014)
[7] M Ghergherehci, H Afarideh, M Ghanadi, A Mohammadzadeh and M Esmailzadeh, *Int. J. Radiat. Res.* **6**, 113 (2008)
[8] A Hossein, A Hager, A Kany, M Nimr and H Ghanim. *Radiat. Eff. Def.* **139**, 163 (1996)
[9] S Akkoyun, *Ann. Nucl. Energy* **55**, 297 (2013)
[10] A Jancar, Z Kopecký, J Dressler, M Veškrna, Z Matěj and C Granja, *Rad. Phys. Chem*. **116**, 60 (2015)
[11] I A Pawelczak, A M Glenn, H P Martinez, M L Carman, N P Zaitseva and S A Payne, *Nucl. Instrum. Methods Phys. Res.* **751**, 62 (2014)
[12] M Takada, S Taniguchi, T Nakamura, N Nakao, Y Uwamino, T Shibata and K Fujitaka, *Nucl. Instrum. Methods Phys. Res.* **476**, 332 (2002)
[13] M Sohrabi and M Katouzi, *Radiat. Prot. Dosimetry* **34**, 149 (1990)
[14] A Majeed, F Humayun, S M Ahmad and S A Durrani, *Radiat. Meas.* **22**, 679 (1993)
[15] M Sadowski, E Mashhadani, A Szydlowski, T Czyzewski, L Gtowacka, M Jaskola and M Wielunski, *Nucl. Instrum. Methods Phys. Res.* **86**, 311 (1994)
[16] F Bahrami, F Mianji, R Faghihi, M Taheri and A Ansarinejad, *Nucl. Instrum. Methods Phys. Res.* **81**, 396 (2016)
[17] SIMNRA/Version-6.06/Max-Planck-Institute fuer Plasma physic company/Germany/www.simnra.com
[18] F Green, G Ramli, S A R Al-Najjar, F Abu-Jarad and S Durrani, *Nucl. Instrum. Methods Phys. Res.* **203**, 551 (1982)
[19] M Taheri, *Procceding of the* 3*rd Iranian Conference on Mach. Vision. Image. Process & Appl*. (2005) Vol. 2, p. 650